Contact capacitance effect in measurement of a.c. impedance spectra for hydrating cement systems

PING XIE, PING GU,
Department of Civil Engineering, University of Ottawa, Ottawa, Ontario, Canada K1N 6N5
J. J. BEAUDOIN
Materials Laboratory, Institute for Research in Construction, National Research Council, Ottawa, Ontario, Canada K1A 0R6

An attempt is made to clarify an argument related to the utilization of a.c. impedance spectroscopy for hydrating cement systems. The question relates to which electrode configuration, 2-point, 3-point or 4-point measurement, is pertinent for impedance spectrum measurement. Theoretical analysis and experiment indicate that these electrode configurations should in principle give the same results. The impedance spectra from 3- or 4-point measurement are, however, strongly influenced by the contact areas between the specimen and potential sensors. This influence is attributed to the potential sensor–specimen "contact capacitance effect". The experiment indicates that when contact capacitance, or area, between the specimen and potential sensor is small enough the impedance spectrum in the Nyquist plot is characterized by an almost perfect semi-circle and negligible high frequency "offset" resistance. These are the typical characteristics of the spectra obtained from 3- and 4-point measurements with point contact between the potential sensors and specimen. The 2-point and 4-point measurements give the same spectra when contact capacitance approaches a sufficiently large value. It is apparent that the impedance spectra from 3- and 4-point measurements with point contact cannot reflect true information about hydrating cement systems. They are experimental artifacts. The 2-point measurements, however, can give more reliable results.

1. Introduction

A.c. impedance spectroscopy techniques have emerged as a powerful tool in cement and concrete science. The pioneering work of McCarter [1] has been followed by extensive research in Canada [2–18] and the United States [19–23]. It has been shown that the a.c. impedance spectroscopy technique is an effective method for the characterization of the microstructure and hydration process in hydrating cement systems [2–9, 12, 17]. The excellent potential of this technique in non-destructive testing of concrete structures has also been demonstrated [8, 11, 18].

A typical impedance spectrum for Portland cement paste with stainless steel electrodes is illustrated in Fig. 1. The impedance spectrum generally includes a high frequency arc and a low frequency arc. The former results from the bulk specimen and the latter from the specimen–electrode interfaces. Some typical characteristics of the high frequency arc are highlighted in Fig. 1. The high frequency arc can be considered as a semi-circle that intercepts the real axis at R_1 and R_b. The semi-circle has a diameter R_2 and is depressed with respect to the real axis by an angle α, referred to as the depression angle. The frequency at the apex of the arc, f_0, for hydrating Portland cement systems is usually a few MHz. The parameters that characterize the impedance spectrum, R_1, R_2 (or R_b), f_0 and α, are pertinent as they are descriptors that can be used to obtain relevant physico-chemical and microstructural information of the cement paste system.

It was postulated on the basis of a theoretical model [5] and experiment [6–9, 14, 15] that the origin of the high frequency arc arises from the existence of solid–liquid interfaces in the system. Some fundamental relationships between the impedance spectrum parameters, microstructural characteristics and pore solution chemistry of the system have been proposed and supported by theory and experiment [5–7], i.e.

$$R_1 = k\frac{1}{1 - k_1(1 - p)} \times \frac{1}{\sigma_1} \quad (1)$$

$$R_2 = k\frac{k_2}{p\langle r\rangle} \times \frac{\delta}{\sigma_f} \quad (2)$$

$$f_0 = \frac{\sigma_f}{2\pi\varepsilon_f\varepsilon_0} \quad (3)$$

where k is a cell constant equal to L/S for the specimen with length L (or distance between electrodes) and cross-sectional area S; k_1 and k_2 are coefficients

0022–2461

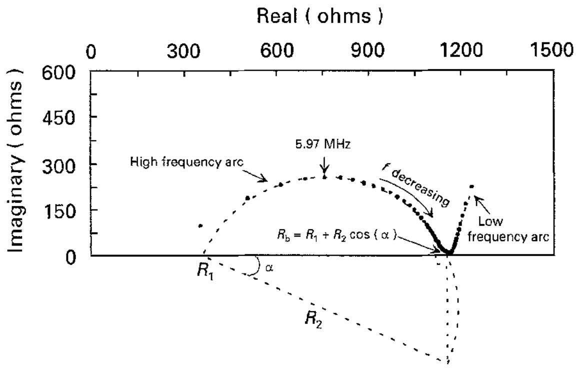

Figure 1 Typical impedance spectrum for Portland cement paste. Portland cement paste, $w/c = 0.30$, 30 days hydration, $L/S = 20$ cm/(7.5 cm × 5.5 cm), room temperature.

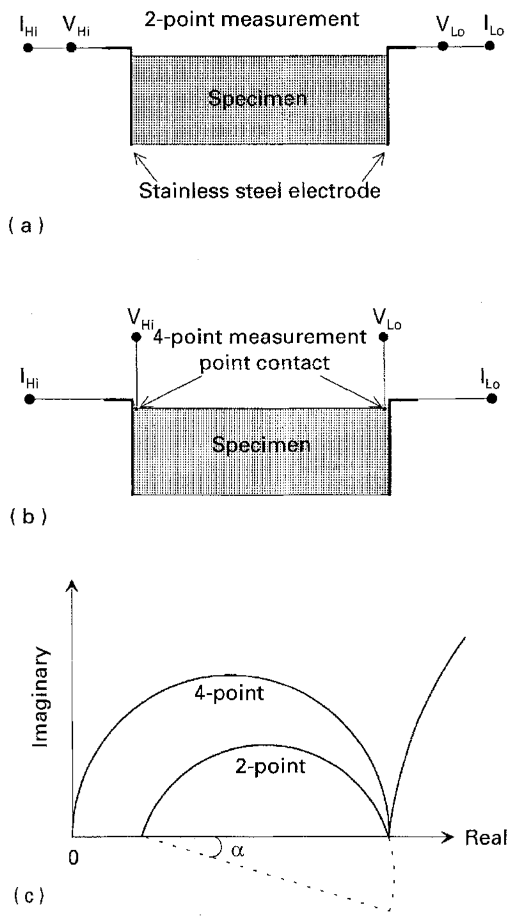

Figure 2 Impedance measurement methods and the corresponding spectra.

dependent on the nature of the solid components and pore geometry; σ_1 is the electrical conductivity of the pore solution; σ_f, ε_f are the electrical conductivity and dielectric constant of solid–liquid interfacial region, respectively; δ is the thickness of the interfacial region; $\varepsilon_0 = 8.85 \times 10^{-12}$ $C^2(Nm^2)^{-1}$ is the permittivity of a vacuum; p and $\langle r \rangle$ are the total porosity and mean pore size of the paste specimen respectively. It can be seen from Equation 1 that for a given cell constant R_1 is mainly governed by the specimen porosity and pore solution conductivity which in turn is a function of the temperature and ionic concentration [6]. R_2 is governed by the porosity and mean pore size as well as the solid–liquid interface parameters, σ_f and δ. The latter are dependent on the ionic concentration of the pore solution [7]. The arc apex frequency, f_0, is mainly governed by the interfacial conductivity. It is also dependent on the ionic concentration of the pore solution. It was suggested on the basis of experiment that the depression angle α reflects to some extent the pore size distribution characteristics. A wider pore size range generally results in a higher α value [2, 16].

The above work is generally based on impedance measurement with the electrode configuration illustrated in Fig. 2a. It is referred to as "2-point" measurement, where the "excitation" electrodes (I_{Hi}, I_{Lo}), facilitating conductance of an a.c. signal through the specimen, and the corresponding potential "sensors" (V_{Hi}, V_{Lo}) are connected at the same points. Recently, American researchers have proposed an alternate electrode configuration ("4-point") for the impedance measurement, Fig. 2b [23]. Planar electrodes are used for providing the a.c. signal in this configuration. The potential sensors are two copper wires whose sharp ends are in contact with the specimen surface. It was found [23] that the impedance spectrum of cement paste using this method was an almost perfect semi-circle with no depression and high frequency "offset" resistance R_1, Fig. 2c. The apex frequency for this semi-circle was generally less than that determined by the "2-point" measurement by approximately one order of magnitude [23]. It was suggested by the US workers that "2-point" measurements, especially the high frequency "offset" resistance R_1 and the depression angle α are possibly experimental artifacts [23]. It was further argued that only multipoint techniques (3- or 4-point) should be used to obtain a valid representation of bulk paste properties such as dielectric constant. It was proposed that existing microstructure-based models incorporating a series equivalent circuit elements corresponding to the high frequency offset resistance be re-evaluated.

The principal objective of this paper is to carefully examine observed differences in the impedance spectra of cement paste determined by the "4-point" measurement and the "2-point" measurement with a view to providing a rational explanation. Questions pertaining to the validity of "4-point" measurement with point-contact between the potential sensors and the specimen are addressed.

2. Theoretical considerations of 2-point and 4-point measurements

A brief review of the basic principles of impedance measurement is relevant. An a.c. signal generated by the instrument is applied to the specimen through the electrodes. I_{Hi} and I_{Lo}, as shown in Fig. 2a and b. The current intensity through the sample, **I**, potential difference between the two potential sensors, **V**, and the phase angle θ are determined. These quantities are expressed as follows:

$$\mathbf{I} = |\mathbf{I}| \exp^{(j\omega t)}, \qquad \mathbf{V} = |\mathbf{V}| \exp^{[j(\omega t + \theta)]} \quad (4)$$

where ω is the angular frequency and t is time. Hence, the impedance $\mathbf{Z}$ can be obtained as follows:

$$\mathbf{Z} = \frac{\mathbf{V}}{\mathbf{I}} = \frac{|\mathbf{V}|}{|\mathbf{I}|}\exp^{(j\theta)} = |\mathbf{Z}|\exp^{(j\theta)} \quad (5)$$

and

$$\mathrm{Re}(\mathbf{Z}) = \frac{|\mathbf{V}|}{|\mathbf{I}|}\cos(\theta); \quad \mathrm{Im}(\mathbf{Z}) = \frac{|\mathbf{V}|}{|\mathbf{I}|}\sin(\theta) \quad (5a)$$

In Equation 5a, $|\mathbf{V}|$, $|\mathbf{I}|$ and θ are three basic quantities that can be directly determined by the instrument. $|\mathbf{I}|$ is usually a constant for a given specimen and instrument settings. $|\mathbf{V}|$ is sensed by the potential sensors, and is obviously dependent on the distance between the sensors. θ is determined by an analyser through comparison of the signal picked up by the potential sensors with that generated by the signal generator. It is apparent that these quantities are theoretically independent of measurement method, i.e. 2- or 4-point, if the distance between the potential sensors is constant. Hence, 2- and 4-point measurements are theoretically supposed to give the same impedance spectrum. The actual difference, however, between 2- and 4-point measurements illustrated in Fig. 2c is so large that further investigation is required.

Experiments using 4-point measurement with point contact between the potential sensors and the specimen surface similar to the American work were repeated. It was confirmed that the impedance spectrum is an almost perfect semi-circle with a negligible high frequency "offset" resistance. It was also found that an increase in the potential sensor–specimen contact area results in a variance of the spectrum from ideal and an increase in the high frequency "offset" resistance. It appears, however, that this was attributed to inductive effects due to interference of the sensors [23]. The following analysis indicates that this is not the case.

Consider the electrical connections in the point-contact 4-point measurement scheme, Fig. 3a, especially the contact point between the potential sensor and sample surface, Fig. 3b. A solid–liquid interface between the sensor and sample containing moisture is always present unlike the case of metal–metal contact. The interface behaves like a capacitor and resistor, referred to as contact capacitor and resistor, in parallel when the impedance measurement is made, Fig. 3c. The contact capacitance C_c is expected to be very small as the contact area for point contact is relatively small. It is estimated to be in the nF range or less. This happens to overlap with the capacitance value resulting in the high frequency arc for hydrating cement systems. Therefore, the existence of the contact capacitor will be reflected in the impedance spectra in the high frequency range. However, if the contact capacitance is large enough, i.e. up to the μF range, equivalent to a larger contact area, the influence of the contact capacitance is not detected in this frequency range.

Experiments supporting the preceding arguments are described as follows.

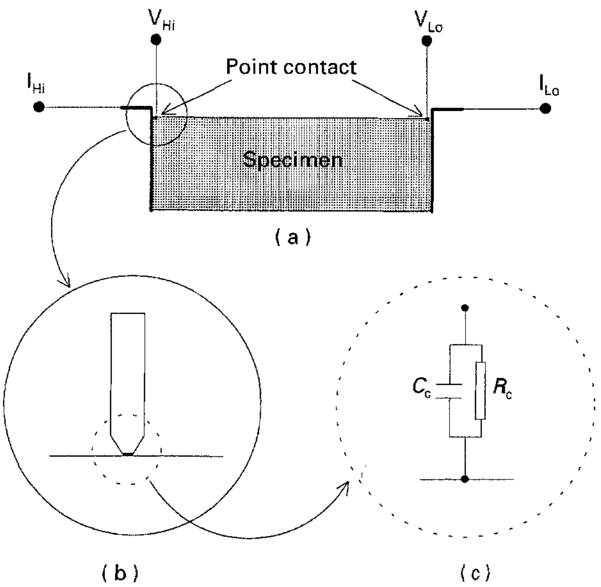

Figure 3 Contact region between the potential sensor and specimen surface and the equivalent circuit.

3. Experimental details

The impedance analyser used was Schlumberger 1260 impedance gain-phase analyser. The excitation amplitude was set to 50 mV. The analyser was operated in the floating, differential input mode. Measurements were made logarithmically down in the frequency range from 30 MHz to 100 Hz with 20 readings per decade.

Two sets of experiments were conducted:

1. The first was conducted on Portland cement paste with *w/c* ratio of 0.30, hydrated 30 days at 100% R.H. (relative humidity). The specimen size was 20 cm × 7.5 cm × 5.5 cm. The 2-point measurement was employed in order to test the influence of the contact capacitance and resistance between the potential sensors and specimen surface on impedance spectra. An equivalent R_c–C_c circuit in parallel was connected between each of the potential sensors and the excitation electrodes, Fig. 4.
2. The second was conducted under similar conditions but the cement paste was replaced by an equivalent circuit consisting of capacitors and resistors, Fig. 5. The specimen is simulated by a 220 Ω resistor connected in series with an *R–C*, 947.5 Ω–110 pF, circuit in parallel.

4. Results and discussion

4.1. Cement paste systems

The effect of the contact capacitance on the impedance spectra of cement paste is demonstrated in Fig. 6a and b. The spectra from 2-point and point-contact 4-point measurements are included for comparison. In the 4-point measurement, the needle-like potential sensors were placed as close as possible to the excitation electrodes to keep the potential sensor distance the same in both the 2- and 4-point measurements. A fixed R_c value, 12 kΩ, was employed.

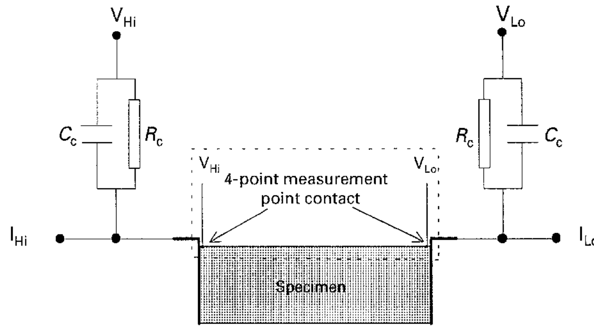

Figure 4 Experimental set-up for testing contact capacitance and resistance effect for cement paste.

Curve	2-point	4-point	1	2	3	4	5	6	7
f_{high} (MHz)	5.97					7.96	7.10	6.32	5.99
f_{low} (kHz)		672	100	89.3	89.3	71.0	56.4	25.2	13.4

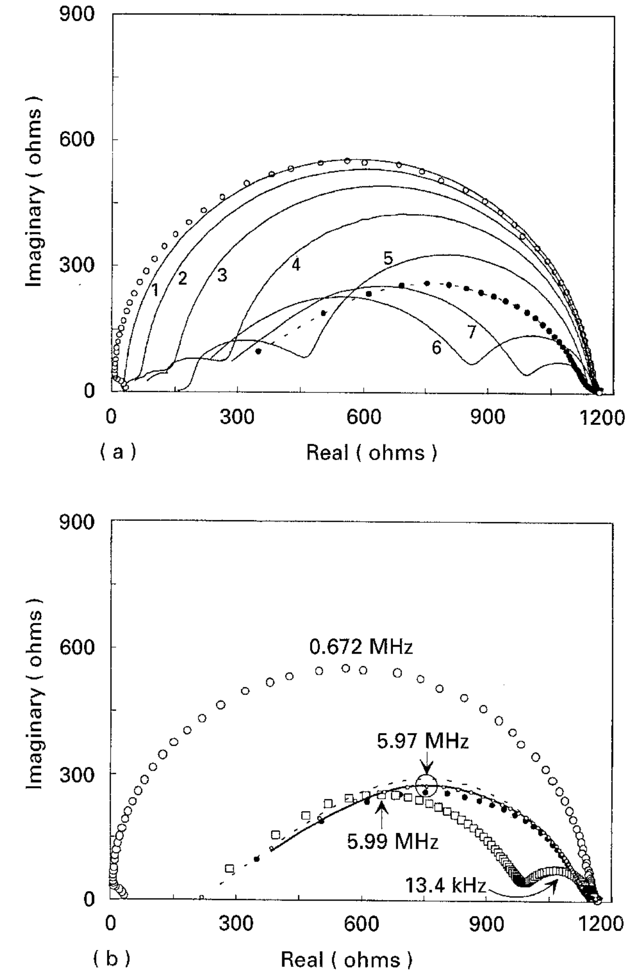

Figure 6 Effect of the contact capacitance on impedance spectra of cement paste. (a) $w/c = 0.30$, 30 days hydration; –•– 2-point; –○– 4-point; 1 4.7 pF, 12 kΩ; 2 10 pF, 12 kΩ; 3 22 pF, 12 kΩ; 4 47 pF, 12 kΩ; 5 100 pF, 12 kΩ; 6 470 pF, 12 kΩ; and 7 1 nF, 12 kΩ. (b) $w/c = 0.30$, 30 days hydration; –•– 2-point; –○– 4-point; –□– 1 nF, 12 kΩ; – – – 10 nF, 12 kΩ; —— 100 nF, 12 kΩ; –◦–1 uF, 12 kΩ.

There are apparently two arcs in different frequency ranges, i.e. relatively high and low frequency, when the contact capacitance C_c ranges from 10 pF to 1 nF, Fig. 6a. The apex frequency for each arc, denoted by f_{high} and f_{low}, respectively, are given in table above Fig. 6a. The value of f_{high} is close to that of the 2-point spectrum and f_{low} is getting close to that of the 4-point spectrum when C_c decreases. It is apparent that the relatively low frequency arc expands with decreasing C_c value and eventually almost overlaps with the 4-point spectrum when C_c equals 4.7 pF. Conversely the relatively high frequency arc increases in size as contact capacitance increases. It eventually overlaps with the 2-point spectrum when C_c is greater than 10 nF, Fig. 6b. The apex frequency of the spectrum is equal to that of the 2-point spectrum.

Examination of the above results, in concert with previous theoretical arguments, leads to the suggestion that the perfect semi-circle with negligible high frequency "offset" observed with 4-point measurement using point contact at the cement paste surface is the result of a very small potential sensor–specimen surface contact area. This tiny contact area is equivalent to the existence of a very small value of C_c in the circuit between the sensors and specimen surface. Thus, point-contact 4-point measurement does not detect real information representing specimen characteristics. It produces artifacts. The contact capacitance, however, does not significantly influence the 2-point spectrum since the contact areas, or

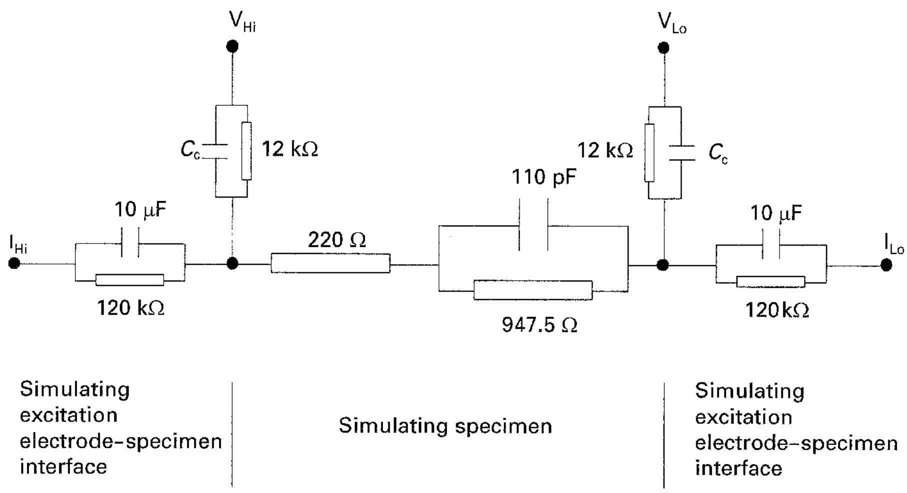

Figure 5 Experimental set-up for testing the effect of capacitance in the contact *R–C* circuit on the impedance spectrum of cement paste simulated by an equivalent *R–C* circuit.

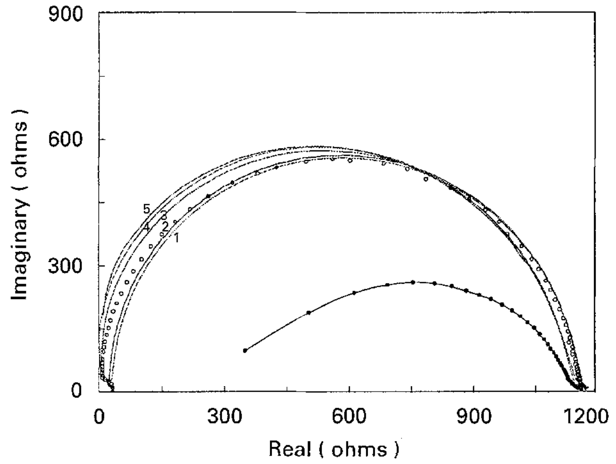

Figure 7 Effect of the contact resistance on impedance spectra of cement paste. $w/c = 0.30$; 30 days hydration (–•– 2-point; –○– 4-point; 1 4.7 pF, 12 kΩ; 2 4.7 pF, 6 kΩ; 3 4.7 pF, 1.2 kΩ; 4 4.7 pF, 0.6 kΩ; 5 4.7 pF, 0.3 kΩ).

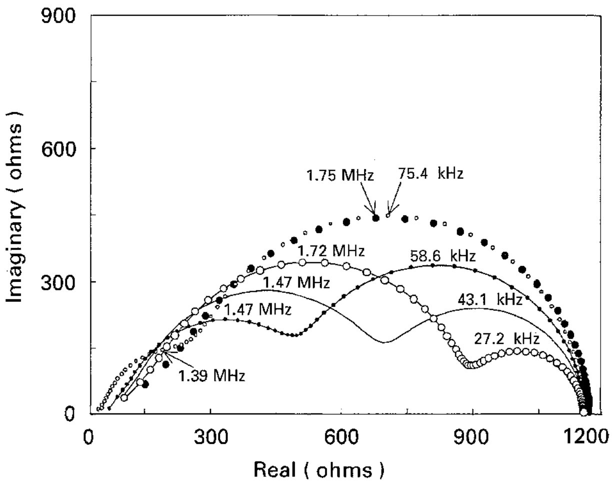

Figure 8 Effect of the contact capacitance on the impedance spectrum when the contact capacitance is comparable with the specimen capacitance –•– 2-point; ——— 220 pF; —○— 47 pF; –○– 470 pF; and —•— 110 pF.

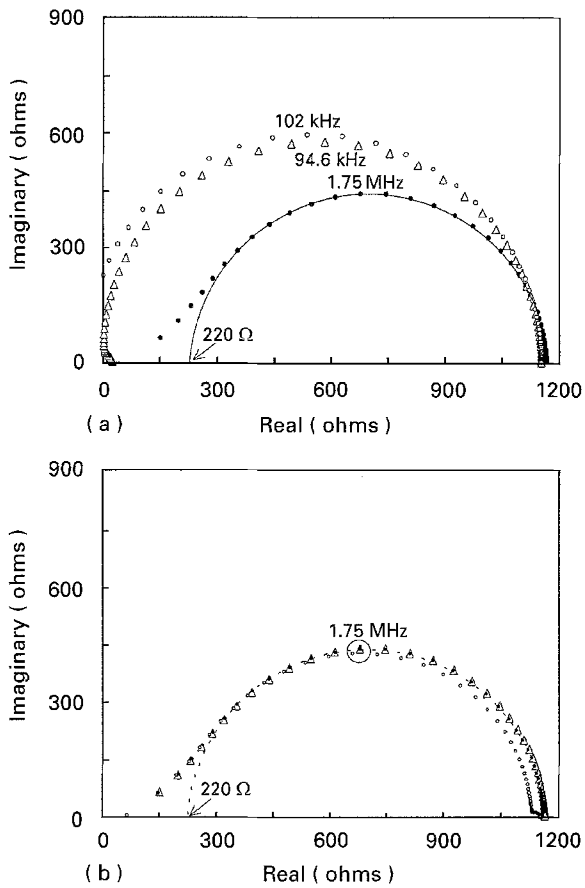

Figure 9 Effect of the contact capacitance on the impedance spectrum when the contact capacitance is much less, (a), or larger, (b), than the specimen capacitance. (a) –•– 2-point; –△– 4.7 pF; and –○– 0 pF. (b) –△– 2-point; –○– 4.7 nF; and –•– 50 nF.

contact capacitance, between the excitation electrodes and specimen are generally sufficiently large.

The effect of the contact resistance on the impedance spectrum is demonstrated in Fig. 7. Contact resistance appears to influence the shape of the arc. The spectrum shifts from the perfect semi-circle when the resistance decreases from 12 kΩ to 300 Ω. An interesting phenomenon occurs near the origin, where the spectrum does not pass through but reverses direction. This phenomenon happens in both 4-point measurement and 2-point measurement with C_c–R_c circuits inserted between the potential sensors and the excitation electrodes. The reason is not clear. However, the results indirectly indicate that the impedance spectrum from 4-point measurement indeed can be simulated by the contact C_c–R_c circuit.

All the spectra in Figs 6 and 7 intercept at the same low frequency point, R_b in Fig. 1. This is understandable since the effect of the contact capacitance and bulk specimen capacitance is not detectable at low frequency. R_b is simply a total sample resistance.

4.2. Capacitor–resistor circuit systems

Impedance spectra for the R–C circuit illustrated in Fig. 5 are plotted in Figs 8 and 9a and b, where the spectrum from 2-point measurement, without the contact capacitors and resistors, is included for comparison. Three cases are represented in Figs 8 and 9a and b and are described as follows:

1. The contact capacitance is comparable with that of the specimen capacitor, 110 pF, Fig. 8. It is apparent that, as in the case of cement paste, the spectra consist of two arcs. The relatively low frequency arc increases in size with decreasing contact capacitance.
2. The contact capacitance is much less than that of the specimen capacitor Fig. 9a. If this is the case, for example $C_c = 4.7$ pF, the relatively high frequency arc disappears. The lower frequency arc dominates and shows all the characteristics, including the "shift back" near the origin, of the spectrum from point-contact 4-point measurement. In an extreme case where the contact capacitors are removed, i.e. $C_c = 0$ pF, the spectrum is still well shaped. It should be emphasized that the theoretical value of the high frequency "offset" resistance R_1 is 220 Ω. This R_1 value, however, vanishes as a result of the contact capacitance effect. It can be obtained, however, with fair precision by simulating the data from the 2-point measurement, Fig. 9a.
3. The contact capacitance is much greater than that of the specimen capacitor, Fig. 9b. If this is the

case, for example $C_c = 50$ nF, the contact capacitance effect is undetectable in the high frequency range. Thus, the spectrum is exactly the same as for 2-point measurement.

In summary, the experimental results for both cement paste and R–C circuit systems indicate that the contact capacitance and resistance between the potential sensors and the specimen strongly influence the impedance spectrum, especially when the contact capacitance is comparable with and much less than the specimen capacitance. This illustrates an important principle for the impedance measurement of solid materials, i.e. point contact between the electrodes and the specimen should be avoided. Otherwise, the results obtained are questionable.

It is not clear why the contact capacitance and resistance can result in a dramatic change in the impedance spectrum. Further research is necessary.

The measured points approaching the high frequency "offset", R_1, from 2-point measurement near the upper-limit of frequency, Fig. 9a, diverge from the theoretical curve. The cause is probably equipment related. However, an R_1 value can be obtained with fair precision by fitting the points on the circular arc. The R_1 value through such fitting is unique as long as the sampling density with respect to frequency is high enough.

5. Conclusions

1. The impedance spectrum measurement for hydrating cement systems is strongly influenced by the contact capacitance and resistance, or contact area, between the potential sensors and the specimen, especially when the contact capacitance is comparable with and much less than the specimen capacitance.

2. A near perfect semi-circle nearly passing through the origin occurs in the Nyquist plot when the contact areas are small enough, e.g. in the case of point contact. Therefore, the impedance spectra obtained by point-contact 4-point measurement do not reveal true specimen information.

3. An important principle for the impedance measurement of solid materials is that point contact between the electrodes and the specimen should be avoided. Otherwise, the results obtained are questionable.

4. Conventional 2-point measurement is a reliable method. The contact capacitance between the electrodes and the specimen is large enough so that it does not influence the features of the high frequency arc in the impedance spectrum of hydrating cement systems.

5. The high frequency "offset" resistance, R_1, of the impedance spectrum from "2-point" measurement can be obtained with fair precision through fitting the measured points on the circular arc, as long as the sampling density with respect to frequency is high enough.

Acknowledgement

The financial support of the Network of Centers of Excellence on High Performance Concrete is gratefully acknowledged.

References

1. W. J. MCCARTER, *Cem. Concr. Res.* **17** (1988) 517.
2. P. GU, P. XIE, J. J. BEAUDOIN and R. BROUSSEAU, *ibid.* **22** (1992) 833.
3. *Idem, ibid.* **23** (1993) 157.
4. P. GU, P. XIE and J. J. BEAUDOIN, *ibid.* **23** (1993) 581.
5. P. XIE, P. GU, Z. Z. XU and J. J. BEAUDOIN, *ibid.* **23** (1993) 359.
6. P. GU, Z. Z. XU, P. XIE and J. J. BEAUDOIN, *ibid.* **23** (1993) 531.
7. Z. Z. XU, P. GU, P. XIE and J. J. BEAUDOIN, *ibid.* **23** (1993) 853.
8. P. GU, Z. Z. XU, P. XIE and J. J. BEAUDOIN, *ibid.* **23** (1993) 675.
9. Z. Z. XU, P. GU, P. XIE and J. J. BEAUDOIN, *ibid.* **23** (1993) 1007.
10. P. GU, Z. Z. XU, P. XIE, J. J. BEAUDOIN and N. M. P. LOW, *Adv. Cem. Res.* **5** (1993) 87.
11. P. GU, P. XIE and J. J. BEAUDOIN, *Cem. Concr. Compos.* **15** (1993) 173.
12. P. GU, P. XIE, J. J. BEAUDOIN and C. JOLICOEUR, *ibid.* **24** (1994) 433.
13. P. GU, P. XIE and J. J. BEAUDOIN, *Adv. Cem. Res.* **5** (1994) 171.
14. P. XIE, P. GU, Y. FU and J. J. BEAUDOIN, *Cem. Concr. Res.* **24** (1994) 704.
15. *Idem, ibid.* **24** (1994) 92.
16. P. GU, P. XIE, Y. FU and J. J. BEAUDOIN, *ibid.* **24** (1994) 86.
17. *Idem, ibid.* **24** (1994) 89.
18. P. GU, P. XIE and J. J. BEAUDOIN, *Cement, Concrete, Aggregates*, **17** (1995) 92.
19. C. A. SCUDERI, T. O. MASON and H. M. JENNINGS, *J. Mater. Sci.* **26** (1991) 349.
20. B. J. CHRISTENSEN, T. O. MASON and H. M. JENNINGS, *J. Amer. Ceram. Soc.* **75** (1992) 939.
21. *Idem, Mater. Res. Soc. Symp. Proc.* **245** (1992) 271.
22. R. T. COVERDALE, E. J. CARBOCZI, H. M. JENNINGS, B. J. CHRISTENSEN and T. O. MASON, *J. Amer Ceram. Soc.* **76** (1993) 1150.
23. S. J. FORD, T. O. MASON, B. J. CHRISTENSEN, R. T. COVERDALE, H. M. JENNINGS and E. J. GARBOCZI, *J. Mater. Sci.* submitted.

Received 1 August 1994
and accepted 17 July 1995